Appendix A
Ab initio Computational Methods

The objective of *ab initio* approaches based on applied quantum theory is to calculate stationary states for electrons in the electrostatic field of nuclei, i.e., the electronic structure (ES). The energy of this ground state can then serve as a potential energy for displacements of nuclei. From the point of view of ideal-strength (IS) calculations, the total energy of the system is the most important output of *ab initio* methods.

The main advantage of *ab initio* methods is their independence of experimental data. Unlike in the case of empirical and semi-empirical methods, there is no need for calibration parameters. Thus, they can also be used for calculation of some structural and mechanical characteristics of hypothetical systems (prediction of properties of materials that have not yet been developed) or study of materials behaviour under large deformations (far from the equilibrium state) that can give a better understanding of micromechanisms of materials failure.

First attempts to develop applicable theories were made in the late 1920s [421, 422], a few years after the foundations of modern quantum theory were laid (derivation of the Schrödinger equation). A very successful step forward was the Hartree–Fock method [422, 423]. This method yields very accurate bond lengths in molecules. On the other hand, the binding energies are generally not in good agreement with experimentally obtained energies. Moreover, for solids, the Hartree–Fock method has problems with a description of band structures. The density functional theory (DFT) [37, 38] was invented to include correlation effects without using the very costly wave function methods. All the methods used within this book are based on the DFT.

In DFT the energy is not obtained as eigenvalues of a wave function, but rather as a functional of the electron density. The complex problem of many interacting electrons is transformed into a much simpler study of single electron interactions with an effective potential U_{eff} created by other electrons and all nuclei. This is expressed by the Kohn–Sham equation (one-electron Schrödinger equation)

$$(-\Delta + U_{eff}(\mathbf{r}) - \varepsilon_i)\psi_i(\mathbf{r}) = 0,$$

where ε_i represents the one-electron energies and ψ_i are the one-electron wave functions.

The wave functions are then occupied in accordance with the Pauli principle and a new field is obtained by solving the Poisson equation for point nuclei shielded by the electronic density

$$\rho(\mathbf{r}) = \sum_{i,occ} |\psi_i(\mathbf{r})|^2 .$$

In the case of periodic crystalline materials, the one-electron wave functions are expanded into appropriate basis sets and satisfy the Bloch theorem. The Kohn–Sham equation is solved iteratively until the solution becomes self-consistent. This means that the electron density, determined from the effective one-electron potential, must generate the same effective potential (which is again a functional of the electron density). The self-consistent cycle usually starts with a guess of the effective potential (superposition of atomic-like potentials) and then the input and output potentials are appropriately mixed before starting a new iteration. The quality and speed of the convergence of such calculations is related not only to the choice of a suitable basis, but also to the sophistication of the iterative process. The necessary corrections for exchange and correlation are also included in the effective potential U_{eff}. This seems to be the crucial point of *ab initio* calculations because the exchange-correlation (XC) functional is not known exactly and must be approximated. The first (and the simplest) attempt to build an approximation of the XC energy functional in the DFT is the local density approximation (LDA) [424]. The LDA is local in the sense that the electron exchange and correlation energy at any point in space is a functional of the electron density at that point only. As a consequence of this, LDA fails in situations where the density undergoes rapid changes (molecules). An improvement to this can be made by considering the gradient of the electron density. The density gradient corrections are implemented in the so-called Generalized Gradient Approximation (GGA). While there is only one LDA there are several different parameterizations of the GGA [425–427].

Nevertheless, it is the choice of the basis wave functions that makes the main difference between various methods used for the ES calculations. The better we choose them (according to the character of the problem), the smaller number of them is needed for the description of one-electron wave functions. Commonly used bases are augmented (APW) and orthogonalized (OPW) plane waves, linear muffin-tin orbitals (LMTO), linear combination of atomic orbitals (LCAO), of Gaussian orbitals (LCGO) and linear augmented Slater-type orbitals (LASTO), augmented spherical waves (ASW), etc. The Korringa–Kohn–Rostoker (KKR) method proceeds by the use of the Green function of the Kohn–Sham equation and is also called Green's func-

tion (GF) method. The pseudopotential approach applied mostly to solids containing no d- or f-electrons is also widely used. A detailed description of these methods may be found in many books and articles, e.g., in [86, 88, 89]. The atomic configurations corresponding to deformed structures usually have lower symmetries and, at the strength limit, they are very far from the lowest-energy equilibrium state. Therefore, to obtain reliable structural energy differences, the full-potential methods (i.e., without any shape approximation of the crystal potential and the electronic charge density) have to be utilized in such studies. At present, several codes are available, e.g., WIEN, VASP, FHI, FLEUR, FPLO, FPLMTO, ABINIT, SIESTA, etc.

All the *ab initio* calculations of IS presented in this book were performed by using the following three computational codes: LMTO-ASA, WIEN and VASP.

A.1 TB-LMTO-ASA Code

Linearized *ab initio* methods have been successfully utilized for solving many problems in materials science [428, 429]. One of the most effective approaches for early first principles calculations was the LMTO formalism which has been continuously developed since 1980 [428–430]. This method is very appropriate for self-consistent calculations.

In the LMTO-ASA code [431], the crystal potential U is approximated by a muffin-tin (MT) shape potential which is composed of a set of spherically symmetric potentials inside slightly overlapping spheres around individual nuclei and a constant potential in the interstitial region outside the spheres (Figure A.1). Atomic-like orbitals derived for the MT potential constitute a suitable basis set. The tight binding approximation, which is also implemented into the code [432], assumes that the full Hamiltonian may be approximated by that of an isolated atom centred at each lattice point. The atomic orbitals (eigenfunctions of the single-atom Hamiltonian) are assumed to be negligible at distances exceeding the lattice constant.

In all presented calculations, the LMTO method is used in the framework of an atomic sphere approximation (ASA) which is particularly suitable for closely packed structures like fcc, hcp or bcc [428]. The size of a spherically symmetric potential is assumed to be equal to that of the Wigner–Seitz cell (Figure A.1(b)). This suppresses the interstitial region and neglects the kinetic energy of related free electrons. Owing to the necessary space-filling condition, ASA represents a physically plausible model only for a description of an infinite system of atomic spheres.

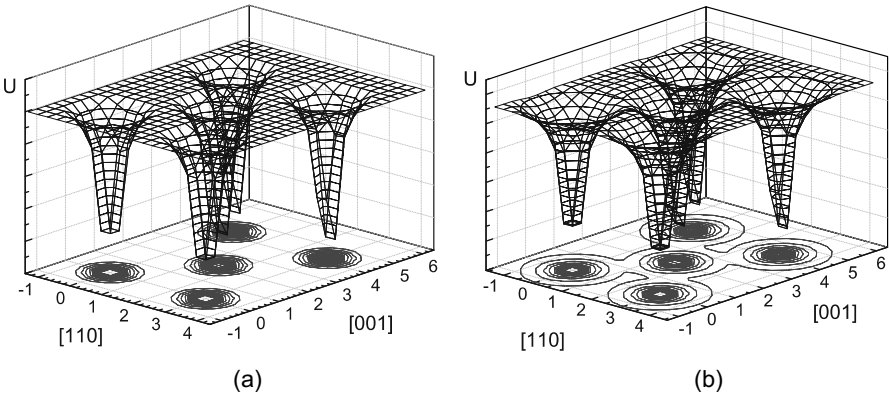

Figure A.1 Muffin-tin shape potential in (110) plane of a general bcc crystal of the lattice constant $a = 3$ au with spherical radii: (a) $r_{MT} = 1$ au, and (b) $r_{MT} = r_{WS} = 1.48$ au

A.2 Wien 95 – w2k Codes

The program package WIEN [433] does not use any shape approximation to the potential. The crystal environment is divided into a region of non-overlapping atomic spheres (centred at individual atomic sites) and an interstitial region as can be seen in Figure A.2. In order to describe ES reliably and effectively, two different basis sets are employed: a product of linear combination of radial functions and spherical harmonics is used inside the spheres whereas the wave functions in the interstitial region are expanded into a linear combination of plane waves. The solution in both regions must be continuous at the spherical boundaries. Each basis function is then defined as a plane-wave in the interstitial region connected smoothly to a linear combination of atomic-like functions in the spheres, thus providing an efficient representation throughout the space. A similar representation is used for potentials and charge densities. The method is called the linear augmented plane wave (LAPW) method [428, 434].

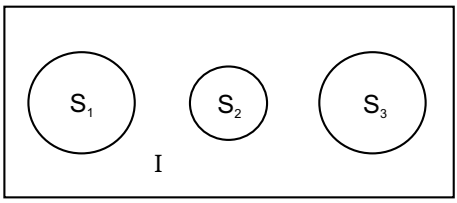

Figure A.2 Illustration of a crystal model – three atomic spheres (S_1 – S_3) with potential $U_S(\mathbf{r}) = \sum_{lm} U_{lm}(r) Y_{lm}(\hat{r})$ embedded in the interstitial region I with $U_I(\mathbf{r}) = \sum_K U_{\mathbf{K}}(r) \mathrm{e}^{i\mathbf{K}\mathbf{r}}$

In order to increase the flexibility of the basis (to improve upon the linearization of wave functions) and to make possible a consistent treatment of semicore and valence states in one energy window (to ensure orthogonality) additional basis functions can be added. They are called local orbitals [435] and consist of a linear combination of two radial functions at two different energies (e.g., at the 3s and 4s energy) and one energy derivative (at one of these energies). The local orbitals are normalized and have zero value and slope at the spherical boundaries.

A.3 VASP Code

Another way of avoiding a problem with plane wave basis set in the vicinity of atomic nuclei, where the number of plane waves would exceed any practical limits (perhaps except for H or Li), is to substitute the exact potential by a pseudopotential.

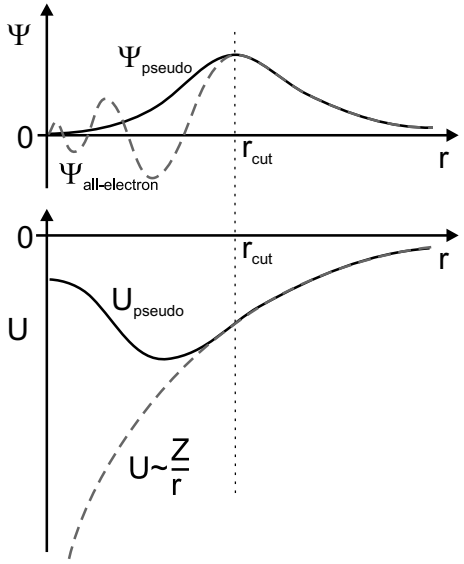

Figure A.3 Comparison of a wavefunction in the Coulomb potential of the nucleus (*dashed lines*) to that in the pseudopotential (*solid lines*)

Construction of the pseudo-wavefunctions is schematically described in Figure A.3. The Coulomb potential of the nucleus and the corresponding wavefunction are represented by dashed lines. The solid line displays the pseudopotential and the pseudo-wavefunction. The real and the pseudo-

wavefunction (and also the potentials) match above a certain cutoff radius r_{cut}.

The pseudopotential approach has been implemented in the VASP (Vienna *ab initio* Simulation Package) code. This code was developed at the Institut für Materialphysik, Universität Wien. The VASP currently supports three types of pseudopotentials: norm-conserving pseudopotentials, ultrasoft pseudopotentials and projector augmented wave pseudopotentials [436–438]. In all three cases, the core electrons (at lower energy levels than valence electrons) are precalculated in an atomic environment and kept "frozen" during the remaining calculations.

Appendix B
Mixed-mode Criteria of Crack Stability

In order to describe the crack stability under mixed-mode loading, various concepts within the framework of LEFM were proposed (e.g., [162–164]). In this brief overview, the stress intensity factors are denoted only by capital letters K_I, K_{II} and K_{III}, as is common for remote quantities. However, the criteria are relevant also to local stress intensity factors usually denoted as k_1, k_2 and k_3.

B.1 Energy Criterion

The criterion postulates that the total energy $G_I+G_{II}+G_{III}$, released by the system to create a unit of a new surface, equals the crack growth resistance G_c:

$$G_c = G_I + G_{II} + G_{III}. \tag{B.1}$$

When the crack grows in its original plane (or propagates in a self-similar manner), the energy criterion can be expressed in terms of the effective K-factor as

$$K_c = \sqrt{K_I^2 + K_{II}^2 + \frac{4}{\kappa+1}K_{III}^2}, \tag{B.2}$$

where K_c is the critical stress intensity factor (fracture toughness), $\kappa = 3-4\nu$ for plane strain, $\kappa = (3-\nu)/(1+\nu)$ for plane stress and ν is the Poisson's ratio.

B.2 Criterion of Linear Damage Accumulation

Each of Equations B.1 and B.2 can be understood as a condition of subsequently reaching the critical level of material damage during loading. If the partial damages accumulate independently, the mixed-mode criterion

$$\frac{G_I}{G_{Ic}} + \frac{G_{II}}{G_{IIc}} + \frac{G_{III}}{G_{IIIc}} \leq 1$$

can be accepted. Clearly, for the special case $G_{Ic} = G_{IIc} = G_{IIIc} = G_c$, the criterion of linear damage accumulation transfers to the energy criterion. Under the dominant mode I loading, the problem of shear friction in modes II and III on the rough fracture surfaces is not crucial due to sufficiently large opening displacements of crack flanks. Consequently, the equality of critical crack driving forces in all modes might be assumed and the energy criterion can be accepted.

Since the assumption of self-similar crack propagation does not hold under a general remote mixed-mode loading, one must be careful when applying both the above-mentioned criteria. They appear to be useful only for a prediction of the moment of unstable fracture or, generally, in the case of a dominant external mode I loading of microscopically tortuous cracks. The description of long fatigue crack propagation under external mixed-mode loading conditions by means of these criteria is rather limited in the sense that the growth direction cannot be predicted.

B.3 Criterion of Minimal Deformation Energy

The deformation energy density S is minimal in those elements near the crack front, where the ratio of the hydrostatic tensile stress and the octahedral stress is maximal [439]. In such elements, therefore, the first local fracture is expected to occur and the crack propagates towards such damaged sites in the matrix. In the plane mixed-mode I+II, the condition of minimal S yields the stability condition as

$$K_{eff}^2 = \frac{16G}{2\,(\kappa - 1)} \left(a_{11}(\theta_m) K_I^2 + 2a_{12}(\theta_m) K_I K_{II} + a_{22}(\theta_m) K_{II}^2 \right),$$

where $a_{ij}(\theta_m)$ are angular functions and G is the shear modulus. The criterion generally enables us to predict the moment of crack nucleation as well as the crack growth direction in the 3D homogeneous continuum. Its disadvantage is a rather low transparency.

B.4 Criterion of Maximal Principal Stress

This criterion can be derived from the energy criterion by expressing the effective crack driving force G_{eff} as a function of growth angle θ and by searching its maximal value. It can be shown that this maximum corresponds to a crack perpendicular to the maximum principal stress. Considering the plane model, stresses in close vicinity of the crack tip can be expressed as follows:

$$\sigma_\theta = \frac{1}{\sqrt{2\pi r}} \cos\frac{\theta}{2}\left(K_I \cos^2\frac{\theta}{2} - \frac{3}{2}K_{II}\sin\theta\right),$$
$$\tau_{r\theta} = \frac{1}{2\sqrt{2\pi r}} \cos\frac{\theta}{2}\left(K_I \sin\theta + K_{II}\left(3\cos\theta - 1\right)\right).$$

If $\tau_{r\theta} = 0$, then the hoop stress σ_θ becomes the principal stress. This condition determines the growth angle θ_m as well as the related effective stress intensity value:

$$\tan\frac{\theta_m}{2} = \frac{K_I}{4K_{II}} \pm \frac{1}{4}\sqrt{\left(\frac{K_I}{K_{II}}\right)^2 + 8},$$

$$K_{eff} = K_I \cos^3\frac{\theta_m}{2} - 3K_{II}\cos^2\frac{\theta_m}{2}\sin\frac{\theta_m}{2}.$$

The criterion can be used for predictions of crack stability and growth in homogeneous materials. The criterion does not involve the antiplane mode III and, consequently, it can be applied only in the framework of 2D models. Nevertheless, a very good applicability of the maximum principal stress criterion to propagation of long fatigue cracks was already proven (e.g., [399,440]). This success can be understood from the micromechanical point of view. Indeed, the fatigue crack tries to maximize the opening as well as the friction between the flanks. Consequently, it inclines to the maximum opening mode I perpendicularly to the maximal main stress direction, thereby also minimizing the shear modes (friction).

Appendix C
Plastic Flow Rate Inside the Neck

C.1 Ideal Model

When taking Equations 2.25, 2.26 and ranges $\lambda_1 \in \langle 0.8, 2\rangle$, $\lambda_2 \in \langle 0, 1\rangle$ into account, the growth of the semi-axes of elliptical voids at the onset of necking can be described as

$$a = a_0 \mathrm{e}^{0.8\varepsilon_p}, \qquad b \approx b_0 \equiv a_0 \tag{C.1}$$

while

$$a = a_0 \mathrm{e}^{2\varepsilon_p}, \qquad b \approx a_0 \mathrm{e}^{\varepsilon_p} \tag{C.2}$$

holds in the final stages of necking just before the final fracture. In order to calculate the active volume V_2, the surface area of the elliptical void S_{el} has to be considered as

$$S_{el} \cong 2\pi \left(b^2 + ab\right). \tag{C.3}$$

By inserting Equations C.1 and C.2 into Equation C.3 and transferring the surface of the ellipsoid to that of the equivalent sphere of the same surface area one obtains

$${}^{a}S_{el} = 4\pi a_0^2 \mathrm{e}^{0,4\varepsilon_p}, \qquad {}^{b}S_{el} = 4\pi a_0^2 \mathrm{e}^{2,5\varepsilon_p}.$$

A corresponding error of this transfer is less than 10% for $0 < \varepsilon_p < 1$. Thus, the variation of the void surface during the necking process can be expressed as

$$S_{el} \approx 4\pi a_0^2 \mathrm{e}^{\kappa\varepsilon_p}, \tag{C.4}$$

where $0.4 < \kappa < 2.5$. Let us denote δ the mean distance from the void surface to the outer boundary of the volume V_2 (see Figure 2.30) and n the number

of voids in V_1. With respect to Equations C.4 and 2.30, where $V_0 = \pi r_0^2 h$, one obtains

$$V_2 \cong 4\pi a_0^2 \delta n \mathrm{e}^{\kappa\varepsilon_p}.$$

By considering Equation 2.30 ($V = V_1$) and denoting $\Theta = \frac{4\pi\gamma a_0^2 \delta n}{V_0}$, $\gamma = 1 + \kappa$ we get

$$\mathrm{d}\left(\frac{V_2}{V_1}\right) \cong \mathrm{d}\left(\frac{4\pi a_0^2 \delta n}{V_0}\,\mathrm{e}^{(1+\kappa)\varepsilon_p}\right) = \Theta \mathrm{e}^{\gamma\varepsilon_p}\mathrm{d}\varepsilon_p. \tag{C.5}$$

When inserting Equation C.5 into Equation 2.33 one obtains

$$\frac{\mathrm{d}f_m}{\mathrm{d}\varepsilon_p} \cong -\Phi f_m + \Theta \mathrm{e}^{\gamma\varepsilon_p},$$

which is a linear differential equation. By solving this equation, a change of the fraction of mobile dislocations during the unstable deformation inside the neck can be expressed in the following form:

$$f_m \cong \exp\left\{\int_0^{\varepsilon_p} -\Phi \mathrm{d}t\right\}\left[f_m^u + \int_0^{\varepsilon_p} \mathrm{e}^{\gamma s} \exp\left\{\int_0^{s} \Phi \mathrm{d}t\right\}\mathrm{d}s\right].$$

Here f_m^u is the relative density of mobile dislocations at the onset of necking. After integration and some algebraic re-arrangement

$$f_m \cong \left(f_m^u \frac{\Theta}{\gamma + \Phi}\right)\mathrm{e}^{-\Phi\varepsilon_p} + \frac{\Theta}{\gamma + \Phi}\mathrm{e}^{\gamma\varepsilon_p}. \tag{C.6}$$

Equation C.6 shows the dependence of the relative density of mobile dislocations on the plastic deformation during the necking process. By introducing Equation C.6 into the general relationship at Equation 2.29 one obtains

$$\dot{\varepsilon}_p = \mu b v_c \left(\rho_u + M\varepsilon_p\right) \exp\left\{-\frac{D_u}{\langle\sigma_s\rangle_k}\right\}\left(\Omega_1 \mathrm{e}^{-\Phi\varepsilon_p} + \Omega_2 \mathrm{e}^{\gamma\varepsilon_p}\right), \tag{C.7}$$

where $\Omega_1 = f_m^u - \frac{\Theta}{\gamma+\bar{\Phi}}$, $\Omega_2 = \frac{\Theta}{\gamma+\bar{\Phi}}$ and $\bar{\Phi} = \frac{H}{\langle\sigma_s\rangle_k}$. Moreover, ρ_u and D_u are the density of dislocations and the friction stress, respectively, at the onset of necking, $\langle\sigma_s\rangle_k$ and $\bar{\Phi}$ are the mean effective stress and the mean value of Φ during the necking process, respectively ($\langle\sigma_s\rangle_k$ is nearly constant). Finally, an appropriate algebraic re-arrangement of Equation C.7 leads to Equation 2.36.

C.2 Real Model

The formation of cavities at secondary phase particles can be described by assuming either the energetic (matrix/particle interphase) or fracture-mechanics (breaking of the particle) criteria. In both cases, the analysis leads to the relation $\sigma_{cr} \propto a^{-1/2}$, where σ_{cr} is the critical applied stress for the cavity nucleation and a is the particle size (e.g., [157,441,442]. Therefore, the total initial surface S_P of nucleated cavities can be determined as

$$S_P \approx 4\pi K_1 \int\limits_{(K_2/\sigma_{cr})^2}^{\infty} a^{-2} \mathrm{d}a. \tag{C.8}$$

Beyond the ultimate stress σ_u, the true stress $\sigma\left(\varepsilon_p\right)$ is nearly a linear function of ε_p [236, 237]:

$$\sigma_{cr} \approx \frac{4}{3}\sigma_u + K_3\varepsilon_p, \tag{C.9}$$

where K_3 is a constant. A combination of Equations C.9 and C.8 gives

$$S_p \approx 4\pi K_1 \int\limits_{\left[\frac{K_2}{(4\sigma_u/3+K_3\varepsilon_p)}\right]^2}^{\infty} a^{-2} \mathrm{d}a. \tag{C.10}$$

Nucleated voids grow according to Equation 2.24 and their total surface area increases in correspondence with Equation C.4. At the moment of reaching the ultimate stress, the total surface area can be estimated by means of Equation C.10 as

$$S_p^u \approx 4\pi K_1 \int\limits_{(3K_2/4\sigma_u)^2}^{\infty} a^{-2} \mathrm{d}a. \tag{C.11}$$

Let us assume small increments of plastic strain $\Delta\varepsilon_p$. Then, with respect to Equation C.4, the total surface area at $\varepsilon_p^* \gg \Delta\varepsilon_p$ can be approximated as follows:

$$\begin{aligned} S_{el} &\approx S_p^u \mathrm{e}^{\kappa\varepsilon_p} + \left(\frac{\mathrm{d}s_p}{\mathrm{d}\varepsilon_p}\right)_0 \mathrm{e}^{\kappa\varepsilon_p}\Delta\varepsilon_p + \ldots \\ &+ \left(\frac{\mathrm{d}S_p}{\mathrm{d}\varepsilon_p}\right)_{\varepsilon_p/2} \mathrm{e}^{\kappa\left(\varepsilon_p^*/2\right)}\Delta\varepsilon_p + \ldots + \left(\frac{\mathrm{d}S_p}{\mathrm{d}\varepsilon_p}\right)_{\varepsilon_p^*} \Delta\varepsilon_p \\ &= S_p^u \mathrm{e}^{\kappa\varepsilon_p^*} + \sum_{k=0}^{\varepsilon_p/\Delta\varepsilon_p} \left(\frac{\mathrm{d}S_p}{\mathrm{d}\varepsilon_p}\right)_{k\Delta\varepsilon_p} \mathrm{e}^{\kappa\left(\varepsilon_p^* - k\Delta\varepsilon_p\right)}\Delta\varepsilon_p. \end{aligned}$$

For $\Delta\varepsilon_p \to 0$ the sum can be replaced by an integral:

$$S_{el} \approx S_p^u \mathrm{e}^{\kappa\varepsilon_p^*} + \int_0^{\varepsilon_p^*} \left(\frac{\mathrm{d}S_p}{\mathrm{d}\varepsilon_p} \right) \mathrm{e}^{\kappa\left(\varepsilon_p^* - \varepsilon_p\right)} \mathrm{d}\varepsilon_p. \tag{C.12}$$

By combining Equations C.11, C.10 and Equation C.12, the total surface area related to the plastic strain ε_p reads

$$S_{el} \approx 4\pi K_1 \left[\mathrm{e}^{\kappa\varepsilon_p} \int_{\left(\frac{3K_2}{4\sigma_u}\right)^2}^{\infty} a^{-2}\mathrm{d}a + \int_0^{\varepsilon_p} \mathrm{e}^{\kappa(\varepsilon_p - e)} \frac{\mathrm{d}}{\mathrm{d}e} \left(\int_{\left[\frac{K_2}{(4/3)\sigma_u + K_3 e}\right]^2}^{\infty} a^{-2}\mathrm{d}a \right) \mathrm{d}e \right]$$

and, after integration, one obtains

$$S_{el} \approx 4\pi \frac{K_1}{K_2^2} \times \\ \times \left[\left(\frac{4}{3}\sigma_u \right)^2 \mathrm{e}^{\kappa\varepsilon_p} + \frac{8}{3\kappa}\sigma_u K_3 \left(\mathrm{e}^{\kappa\varepsilon_p} - 1 \right) + \frac{2}{\kappa} \left(K_3 \right)^2 \left(\frac{1}{\kappa}\mathrm{e}^{\kappa\varepsilon_p} - \frac{1}{\kappa} - \varepsilon_p \right) \right]. \tag{C.13}$$

Since, for metallic materials, $K_3 < \frac{4}{3}\sigma_u$, $0.4 < \kappa < 2.5$ and

$$\frac{1}{\kappa}\mathrm{e}^{\kappa\varepsilon_p} = \frac{1}{\kappa} + \varepsilon_p + \frac{1}{2}\kappa\varepsilon_p^2 + \ldots,$$

the last term in the brackets can be neglected ($\varepsilon_p < 1$). After a simple re-arrangement of Equation C.13 (the constant $\frac{2}{3}\sigma_u + \frac{K_3}{\kappa}$ is not too much different from σ_u) one finally obtains

$$S_{el} = 2\pi K_1 \frac{1}{a_{0p}} \left(3\mathrm{e}^{\kappa\varepsilon_p} - 1 \right), \tag{C.14}$$

where $a_{0p} = \left(\frac{3K_2}{4\sigma_u}\right)^2$ is the size of voids that nucleate when reaching the ultimate stress.

Let us further consider that the initial void size is determined by a distribution function of particle sizes and, during the deformation, the number of nucleated voids increases. According to Bergh [443] and other authors (e.g., [444, 445]), the distribution function can be written as

$$g(a) = \frac{1}{a^4}, \qquad a \geq a^*,$$

where a^* is a critical size of particles which start to nucleate voids. Consequently, the total number of particles which, at a given strain, have already nucleated voids reads

$$h(a) = K_1 \int_{a_n}^{\infty} \frac{1}{a^4} \mathrm{d}a, \tag{C.15}$$

where K_1 is a constant, a_n is the smallest size of particles that nucleate voids in a particular deformation stage ε_p. With respect to Equations C.14 and C.15, the dependence of the volume V_2 on the plastic strain is ε_p:

$$V_2 \approx 2\pi K_1 \frac{\delta}{a_{0p}} \left(3\mathrm{e}^{\kappa\varepsilon_p} - 1\right). \tag{C.16}$$

When inserting Equation C.16 into Equation 2.33, and following the same reasoning as in the case of the ideal model, one finally obtains the strain rate formula

$$\begin{aligned} \dot{\varepsilon}_p \approx{}& \mu b v_c \left(\rho_u + M\varepsilon_p\right) \exp\left\{-\frac{D_u}{\langle\sigma_s\rangle_k}\right\} \\ &\left[f_{om}^u - \Theta^* \left(\frac{1}{\gamma + \bar{\Phi}} - \frac{1}{3\gamma\left(1+\bar{\Phi}\right)}\right) \mathrm{e}^{-\Phi\varepsilon_p} + \right. \\ &\left. + \Theta^* \left(\frac{1}{\gamma + \bar{\Phi}} \mathrm{e}^{\kappa\varepsilon_p} - \frac{1}{3\gamma\left(1+\bar{\Phi}\right)}\right) \mathrm{e}^{\varepsilon_p}\right], \end{aligned} \tag{C.17}$$

where $\Theta^* = \frac{6\pi K_1 \delta\gamma}{a_{0p} V_0}$.

Since $\bar{\Phi} > 1$ (H in units of GPa and $\langle\sigma_s\rangle_k$ in hundreds of MPa) and $1.4 < \gamma < 3.5$, the terms $\frac{1}{3\gamma\left(1+\bar{\Phi}\right)}$ in both brackets can be neglected and Equation C.17 reduces to Equation C.7 (both the ideal and the real model lead to a similar result).

List of Reprinted Figures

- Figure 1.17 on page 44 is reprinted from the paper Černý M, Pokluda J, The Theoretical Tensile Strength of fcc Crystals Predicted from Shear Strength Calculations. Journal of Physics: Condensed Matter 21:145406, Fig. 1, © 2009 Institute of Physics and IOP Publishing Ltd.
- Figure 1.24 on page 65 is reprinted from the paper Horníková J, Černý M, Šandera P, Pokluda J, Onset of Microplasticity in Copper Crystal during Nanoindentation. Key Engineering Materials 348–349:801–804, Fig. 1, © 2007 Trans Tech Publications Inc.
- Figure 1.25 on page 66 is reprinted from the paper Horníková J, Černý M, Šandera P, Pokluda J, Onset of Microplasticity in Copper Crystal during Nanoindentation. Key Engineering Materials 348–349:801–804, Fig. 2, © 2007 Trans Tech Publications Inc.
- Figure 2.1 on page 76 is reprinted from the paper Pokluda J, Šandera P, Horníková J, Statistical Approach to Roughness-Induced Shielding Effects. Fatigue & Fracture Engineering Materials & Structures 27:141–157, Fig. 2, © 2004 John Wiley & Sons, Inc.
- Figure 2.3 on page 82 is reprinted from the paper Kotoul M, Pokluda J, Šandera P, Dlouhý I, Chlup Z, Boccaccini A, Toughening Effects Quantifications in Glass Matrix Composite Reinforced by Alumina Platelets. Acta Materialia 56:2908–2918, Fig. 2, © 2008 Elsevier B.V.
- Figure 2.4 on page 83 is reprinted from the paper Kotoul M, Pokluda J, Šandera P, Dlouhý I, Chlup Z, Boccaccini A, Toughening Effects Quantifications in Glass Matrix Composite Reinforced by Alumina Platelets. Acta Materialia 56:2908–2918, Fig. 3, © 2008 Elsevier B.V.
- Figure 2.5 on page 83 is reprinted from the paper Kotoul M, Pokluda J, Šandera P, Dlouhý I, Chlup Z, Boccaccini A, Toughening Effects Quantifications in Glass Matrix Composite Reinforced by Alumina Platelets. Acta Materialia 56:2908–2918, Fig. 6, © 2008 Elsevier B.V.
- Figure 2.11 on page 93 is reprinted from the paper Pokluda J, Šandera P, Horníková J, Statistical Approach to Roughness-Induced Shielding Effects.

Fatigue & Fracture Engineering Materials & Structures 27:141–157, Fig. 10, © 2004 John Wiley & Sons, Inc.

- Figure 2.13 on page 95 is reprinted from the paper Pokluda J, Šandera P, Horníková J, Statistical Approach to Roughness-Induced Shielding Effects. Fatigue & Fracture Engineering Materials & Structures 27:141–157, Fig. 11, © 2004 John Wiley & Sons, Inc.
- Figure 2.20 on page 103 is reprinted from the paper Šandera P, Pokluda J, Horníková J, Vlach B, Lejček P, Jenko M, Fracture of Polycrystalline Fe-2.3%V-0.12%P Alloy. Engineering Fracture Mechanics 77:385–392, Fig. 2, © 2010 Elsevier B.V.
- Figure 2.22 on page 105 is reprinted from the paper Šandera P, Pokluda J, Horníková J, Vlach B, Lejček P, Jenko M, Fracture of Polycrystalline Fe-2.3%V-0.12%P Alloy. Engineering Fracture Mechanics 77:385–392, Fig. 5, © 2010 Elsevier B.V.
- Figure 2.24 on page 106 is reprinted from the paper Šandera P, Pokluda J, Horníková J, Vlach B, Lejček P, Jenko M, Fracture of Polycrystalline Fe-2.3%V-0.12%P Alloy. Engineering Fracture Mechanics 77:385–392, Fig. 7, © 2010 Elsevier B.V.
- Figure 2.25 on page 107 is reprinted from the paper Šandera P, Pokluda J, Horníková J, Vlach B, Lejček P, Jenko M, Fracture of Polycrystalline Fe-2.3%V-0.12%P Alloy. Engineering Fracture Mechanics 77:385–392, Fig. 3, © 2010 Elsevier B.V.
- Figure 3.35 on page 183 is reprinted from the paper Pokluda J, Šandera P, Horníková J, Analysis of Roughness-Induced Crack-Tip Shielding in Terms of Size Ratio Effect. Journal of ASTM International 2:1–15 (JAI11997), Fig. 5, © 2005 ASTM International.
- Figure 3.41 on page 192 is reprinted from the paper Pokluda J, Pippan R, Can a Pure Mode III Fatigue Loading Contribute to Crack Propagation in Metallic Materials? Fatigue & Fracture Engineering Materials & Structures 28:179–186, Fig. 3, © 2005 John Wiley & Sons, Inc.
- Figure 3.42 on page 193 is reprinted from the paper Pokluda J, Pippan R, Can a Pure Mode III Fatigue Loading Contribute to Crack Propagation in Metallic Materials? Fatigue & Fracture Engineering Materials & Structures 28:179–186, Fig. 4, © 2005 John Wiley & Sons, Inc.
- Figure 3.44 on page 196 is reprinted from the paper Pokluda J, Pippan R, Can a Pure Mode III Fatigue Loading Contribute to Crack Propagation in Metallic Materials? Fatigue & Fracture Engineering Materials & Structures 28:179–186, Fig. 7, © 2005 John Wiley & Sons, Inc.
- Figure 3.45 on page 197 is reprinted from the paper Pokluda J, Pippan R, Can a Pure Mode III Fatigue Loading Contribute to Crack Propagation in Metallic Materials? Fatigue & Fracture Engineering Materials & Structures 28:179–186, Fig. 8, © 2005 John Wiley & Sons, Inc.
- Figure 3.50 on page 204 is reprinted from the paper Pokluda J, Trattnig G, Martinschitz C, Pippan R, Straightforward Comparison of Fatigue Crack

Growth under Modes II and III. International Journal of Fatigue 30:1498–1506, Fig. 3, © 2008 Elsevier B.V.

- Figure 3.51 on page 205 is reprinted from the paper Pokluda J, Trattnig G, Martinschitz C, Pippan R, Straightforward Comparison of Fatigue Crack Growth under Modes II and III. International Journal of Fatigue 30:1498–1506, Fig. 1, © 2008 Elsevier B.V.
- Figure 3.53 on page 208 is reprinted from the paper Pokluda J, Trattnig G, Martinschitz C, Pippan R, Straightforward Comparison of Fatigue Crack Growth under Modes II and III. International Journal of Fatigue 30:1498–1506, Fig. 14, © 2008 Elsevier B.V.
- Figure 3.68 on page 226 is reprinted from the paper Slámečka K, Pokluda J, Ponížil P, Major Š, Šandera P, On the Topography of Fracture Surfaces in Bending-torsion Fatigue. Engineering Fracture Mechanics 75:760–767, Fig. 8, © 2008 Elsevier B.V.
- Figure 3.69 on page 230 is reprinted from the paper Slámečka K, Pokluda J, Kianicová M, Major Š, Dvořák I, Quantitative Fractography of Fish-Eye Crack Formation under Bending-Torsion Fatigue. International Journal of Fatigue 32:921–928, Fig. 2, © 2010 Elsevier B.V.
- Figure 3.71 on page 231 is reprinted from the paper Slámečka K, Pokluda J, Kianicová M, Major Š, Dvořák I, Quantitative Fractography of Fish-Eye Crack Formation under Bending-Torsion Fatigue. International Journal of Fatigue 32:921–928, Fig. 4, © 2010 Elsevier B.V.
- Figure 3.72 on page 233 is reprinted from the paper Slámečka K, Pokluda J, Kianicová M, Major Š, Dvořák I, Quantitative Fractography of Fish-Eye Crack Formation under Bending-Torsion Fatigue. International Journal of Fatigue 32:921–928, Fig. 6, © 2010 Elsevier B.V.
- Figure 3.76 on page 236 is reprinted from the paper Slámečka K, Pokluda J, Kianicová M, Major Š, Dvořák I, Quantitative Fractography of Fish-Eye Crack Formation under Bending-Torsion Fatigue. International Journal of Fatigue 32:921–928, Fig. 9, © 2010 Elsevier B.V.

References

1. Kelly A, Macmillan M H (1986) Strong Solids. Clarendon Press, Oxford
2. Raabe D (1998) Computational Materials Science: The simulation of Materials, Microstructures and Properties. Willey-VCH Verlag GmbH, Weinheim
3. Vitek V, Perrin R C, Bowen D K (1970) Phil Mag 21:1049–1073
4. Vitek V (1974) Cryst Lat Defects 5:1–34
5. Gröger R, Bailey A G, Vitek V (2008) Acta Mater 56:5401–5411
6. Paidar V, Pope D P, Vitek V (1984) Acta Metall 32:435–448
7. Gröger R, Vitek V (2008) Acta Mater 56:5426–5439
8. Weertman J (1996) Dislocation Based Fracture Mechanics. World Scientific, Singapore
9. Riemelmoser F O, Pippan R, Stüwe H P (1997) Int J Fract 85:157–168
10. Pippan R, Strobl G, Kreuzer H, Motz C (2004) Acta Mater 52:4493–4502
11. Pokluda J, Pippan R (2007) Mat Sci Eng A462:355–358
12. Pippan R, Kreuzer H G M, Kiener D, Rester M, Motz C (2007) Size Effect in Plastic Deformation and Fracture. In: Šandera P (ed) Materials Structure & Micromechanics of Fracture (MSMF-5). VUTIUM, Brno
13. Brenner S S, (1956) J Appl Phys 27:1484–1492
14. Nadgorny E M, (1962) Sov Phys Usp 5:462–469
15. Bahr D F, Kramer D E, Gerberich W W (1998) Acta Mater 46:3605–3612
16. Woodcock C L, Bahr D F (2000) Scripta Mater 43:783–788
17. Gouldstone A, Koh H J, Zeng K Y, Giannakopoulos A E, Suresh S (2000) Acta Mater 48:2277–2296
18. De la Fuente O R, Zimmerman J A, Gonzales M A, De la Figuera J, Hamilton J C, Pai W W, Rojo J M (2002) Phys Rev Lett 88:036101
19. Jokl M L, Vitek V, McMahon C J Jr (1980) Acta Metall 28:1479–1488
20. Kroupa F (1981) Theoretical strength. In: Pokluda J, Staněk P (eds) Prediction of Mechanical Properties of Metallic Materials by means of Structural Characteristics. ČSVTS, Brno (in Czech)
21. Thomson R (1986) Solid State Phys 39:1–129
22. Huang H, Gerberich W W (1992) Acta Metall Mater 40:2873–2881
23. Kelly A, Tyson W R, Cottrell A H (1967) Phil Mag 15:567–585
24. Pokluda J, Šandera P (1991) Phys Stat Solidi b167:543–50
25. Pokluda J, Šandera P (1994) Key Eng Mater 97–98:467–481
26. Goldschmidt D (1994) Single crystal blades. In: Coutsouradis D *et al.* (eds) Materials for Advanced Power Engineering: Part I. Kluwer Academic Publisher, Dodrecht
27. Frenkel J (1926) Z Phys 37:572–609
28. Polany M (1921) Z Phys 7:323–327

29. Orowan E (1949) Rep Progr Phys 12:185–232
30. Kelly A (1973) Strong Solids. Clarendon Press, Oxford
31. Šandera P, Pokluda J (1993) Scr Metall Mater 29:1445–1451
32. Paxton A T, Gumbsch P, Methfessel M (1991) Phil Mag Lett 63:267–274
33. Macmillan N H (1983) Ideal Strength. In: Latanision R M, Pickens J R (eds) Atomistics of Fracture. Plenum Press, New York
34. Pokluda J, Šandera P (1989) Phys Stat Solidi b151:85–91
35. Pokluda J, Šandera P (1990) Phys Stat Solidi b160:89–95
36. Šandera P, Pokluda J (1994) Metall Mater 32:180–193
37. Hohenberg P, Kohn W (1964) Phys Rev B136:864–871
38. Kohn W, Sham L J (1965) Phys Rev A140:1133–1139
39. Esposito E, Carlson A E, Ling B D, Ehrenreich H, Gelatt C D Jr (1980) Phil Mag A41:251–259
40. Price D L, Cooper B R, Wills J M (1992) Phys Rev B46:11368–11375
41. Šob M, Wang L G, Vitek V (1997) Mat Sci Eng A234–236:1075–1089
42. Šob M, Wang L G, Vitek V (1998) Metall Mater 36:145–158
43. Friák M, Šob M, Vitek V (2003) Phil Mag 83A:3529–3537
44. Kitagawa H, Ogata S (1999) Key Eng Mater 161–163:443
45. Ogata S, Kitagawa H (1999) Comp Mat Sci 15:435–440
46. Li W X, Wang T C(1999) Phys Rev B59:3993–4001
47. Telling R H, Pickard C J, Payne M C, Field J E (2000) Phys Rev Lett 84:5160–5163
48. Roundy D, Cohen M L (2001) Phys Rev B64:212103–212105
49. Luo W, Roundy D, Cohen M L, Morris J W Jr (2002) Phys Rev B66:094110
50. Ogata S, Hirosaki N, Kocer C, Kitagawa H (2001) Phys Rev B64:172102
51. Kocer C, Hirosaki N, Ogata S (2003) Phys Rev B67:035210
52. Xu W, Moriarty J A (1996) Phys Rev B54:6941–6951
53. Söderlind P, Moriarty J A (1998) Phys Rev B57:10340–10350
54. Jhi S H, Louie S G, Cohen M L, Morris J W Jr (2001) Phys Rev Lett 87:075503
55. Ogata S, Li J, Yip S, (2002) Science 298:807–811
56. Roundy D, Krenn C R, Cohen M L, Morris J W Jr (1999) Phys Rev Lett 82:2713–2716
57. Roundy D, Krenn C R, Cohen M L, Morris J W Jr (2001) Phil Mag A81:1725–1747
58. Černý M (2007) Mater Sci Eng A462:432–435
59. Černý M, Pokluda J (2008) Comp Mater Sci 44:127–130
60. Šandera P, Pokluda J, Wang L G, Šob M (1997) Mater Sci Eng A234/236:370–372
61. Černý M, Pokluda J, Šob M, Friák M, Šandera P (2003) Phys Rev B67:035116
62. Černý M, Pokluda J (2004) J Alloys Comp 378:159–162
63. Son Y, Yang R, Li D, Wu W T, Guo Z X (1999) Phys Rev B59:14220–14225
64. Born M (1940) Proc Camb Philos Soc 36:160–172
65. Born M, Fürth R (1940) Proc Camb Phil Soc 36:454–465
66. Hill R, Milstein F (1977) Phys Rev B15:3087–3096
67. Li W X, Wang T C (1998) J Phys: Cond Matter 10:9889–9904
68. Černý M, Šob M, Pokluda J, Šandera P (2004) J Phys: Cond Matter 16:1045–1052
69. Finnis M W, Sinclair J E (1984) Phil Mag A50:45–55
70. Aoki M, Nguyen-Manh D, Pettifor D, Vitek V (2007) Progr Mater Sci 52:154–195
71. Chantasiriwan S, Milstein F (1996) Phys Rev B53:1408–14088
72. Cawkwell M, Woodward C, Nguyen-Manh D, Pettifor D, Vitek V (2007) Acta Mater 5:161–169
73. Ackland G J, Mendelev M I, Stolovitý D J, Han S, Barashev A V (2004) J Phys Cond Matter 16:S2629–S2642

74. Clatterbuck D M, Chrzan D C, Morris J W Jr (2002) Phil Mag Lett 82:141–147
75. Dean D W, Wentzcovitch R M, Keskar N, Chelikowsky J R, Binggeli N (2000) Phys Rev B61:3303–3309
76. Ma Y, Tse J S, Klug D D (2003) Phys Rev B67:140301
77. Horsfield A P *et al.* (2008) Comp Mater Sci 44:16–20
78. Milstein F, Chantasiriwan S (1998) Phys Rev B58:6006–6018
79. Milstein F, Hill R (1979) Phys Rev Lett 43:1411–1413
80. Milstein F, Rasky D J (1996) Phys Rev B54:7016–7025
81. Murnaghan F D (1951) Finite deformation of an elastic solid. John Willey & Sons, New York
82. Nye J F (1985) Physical Properties of Crystals: Their Representation by Tensors and Matrices. Oxford University Press, USA
83. Pokluda J, Černy M, Šandera P, Šob M (2004) J Comp Aid Mater Design 11:1–28
84. Barron T H K, Klein M L (1965) Proc Phys Soc Lond 85:523–532
85. Morris J W, Krenn C R (2000) Phil Mag A80:2827–2840
86. Mehl J M, Klein B M, Papaconstantopoulos D (1994) First principles calculations of elastic properties of metals. In: Westbrook J H, Fleisher R L (eds) Intermetallic Compounds. John Willey & Sons, New York
87. Kim K Y (1999) Phys Rev B54:6245–6254
88. Deutsch T, Lancon F (2003) J Phys Cond Matter 15:1813–1826
89. Harrison W A (2004) Elementary Electronic Structure. World Scientific Publishing, Singapore
90. Craievich P J, Weinert M, Sanchez J M, Watson R E (1994) Phys Rev Lett 72:3076–3079
91. Paidar V, Wang L G, Šob M, Vitek V (1999) Modell Simul Mater Sci 7:369–381
92. Wang J, Li J, Yip S, Phillpot S R, Wolf D (1995) Phys Rev B52:12627–12635
93. Zhou Z, Joós B (1996) Phys Rev B54:3841–3850
94. Yip S, Li J, Tang M, Wang J (2001) Mater Sci Eng A317:236–240
95. Wallace D C (1972) Thermodynamics of Crystals. John Wiley & Sons, New York-London-Sydney-Toronto
96. Li J, Zhua T, Yip S, Van Vliet K J, Suresh S (2004) Mater Sci Eng A365:25–30
97. Černý M, Šandera P and Pokluda J (2001) *Ab initio* Modelling Deformation of Perfect Cubic Crystals under Triaxial Tension. In: Šandera P (ed) MSMF3. VUTIUM, Brno
98. Černý M, Pokluda J (2007) Phys Rev B76:024115
99. Ogata S, Li J, Hirosaki N, Shibutani Y, Yip S (2004) Phys Rev B70:104104
100. Song Y, Xu D S, Yang R, Li D, Wu W T, Guo Z X (1999) Mater Sci Eng A260:269
101. Clatterbuck D M, Krenn C R, Cohen M L, Morris J W Jr (2003) Phys Rev Lett 91:135501
102. Černý M, Pokluda J (2009) J Phys: Cond Matter 21:145406
103. Černý M, Pokluda J (2007) Mater Sci Eng A483–484:692–695
104. Černý M, Šandera P and Pokluda J (1999) Czech J Phys B49:1495–1501
105. Morris J W Jr, Krenn D, Roundy D, Cohen M L (2000) Phase transformations and evolution in materials In: Turchi P E, Gonis A (eds) Hume-Rothery Symp in honor of A G Khatchaturyan. TMS, Warrendale PA
106. Umeno Y, Černý M (2008) Phys Rev B77:100101
107. Černý M, Pokluda J, Šandera P (2004) Mater Sci Eng A 387/389:923–925
108. Šob M, Friák M, Legut D, Fiala J, Vitek V (2004) Mat Sci Eng A387/389:148–157
109. Šob M, Wang L G, Vitek V (1998) Phil Mag B78:653–662
110. Söderlind P, Moriarty J A, Wills J M (1996) Phys Rev B53:14063–14072
111. Wang F M, Ingalls R (1998) Phys Rev B57:5647–5654

112. Friák M, Šob M, Vitek V (2003) Phys Rev B68:184101
113. Milstein F, Farber B, (1980) Phil Mag A42:19–29
114. Mikhailovskii I M, Poltinin I Y, Fedorova L I (1981) Sov Phys Solid State 23:757
115. Šesták P, Černý M, Pokluda J (2007) Mater Sci Eng A481–482:247–249
116. Černý M, Pokluda J (2006) Influence of Superimposed Normal Loading on the Shear Strength in bcc Metals. In: Multiscale Materials Modelling. Freiburg Germany
117. Černý M, Pokluda J (2007) Phys Rev B76:024115
118. Černý M, Pokluda J (2008) A Simple Prediction of the Theoretical Tensile Strength of Cubic Crystals based on the Shear Strength Calculations. In: Pokluda J, Lukáš P, Šandera P, Dlouhý I (eds) Multilevel Approach to Fracture of Materials, Components and Structures (ECF17). Vutium, Brno
119. Černý M, Pokluda J (2010) Acta Mater 58:3117–3123
120. Krenn C R, Roundy D, Morris J W Jr, Cohen M L (2001) Mater Sci Eng A317:44–49
121. Holiday L (1966) Composite Materials. Elsevier, Amsterdam-London-NewYork
122. Černý M, Pokluda J (2006) *Ab initio* study of elasticity and strength of nanofibre reinforced composites. In: Gdoutos E (ed) 16th European Conference of Fracture. Springer
123. Černý M, Pokluda J (2006) Elasticity and strength of nanofibre reinforced composites from first principles. In: 12th European Conference on Composite Materials. Biarritz, France
124. Černý M, Pokluda J (2006) First principles study of of vanadium based composites reinforced by tungsten nanofibres. In: Šandera P (ed) Nano 06. Vutium, Brno
125. Vosko S H, Wilk L, Nusair M (1980) Can J Phys 58:1200–1207
126. Kittel C (1976) Introduction to Solid State Physics. John Wiley & Sons, New York
127. Simmons G, Wang H (1971) Single Crystal Elastic Constants and Calculated Aggregate Properties: A Handbook. MIT Press, Cambridge
128. Černý M, Pokluda J (2009) Elasticity and Strength of Nano-Fibre Reinforced Composites from First Principles. In: Elboujdaini M (ed) 12th International Conference on Fracture (ICF12). NRC, Ottawa, Canada
129. Goodwin L, Needs R, Heine V (1988) Phys Rev Lett 60:2050–2053
130. Huang Y M, Spence J C H, Sankey O F (1994) Phil Mag 70:53–59
131. Haydock R (1981) J Phys 14C:3807–3816
132. Šesták P (2009) Microstructural and mechanical characteristics of NiTi alloy from first principles. PhD Thesis, Brno University of Technology, Brno
133. Neuber H (1958) Kerbspannungslehre. Springer Verlag, Berlin
134. Rice J R, Thomson R (1974) Phil Mag 29:73–79
135. Rice J R, Beltz G E, Sun Y (1992) Peierls Framework for Dislocation Nucleation from a Crack Tip. In: Argon A S (ed) Topics in Fracture and Fatigue. Springer, Berlin
136. Pokluda J, Šandera P (1995) Metall Mater 33:375–383 (in Czech)
137. Ewalds H L, Wanhill R J H (1989) Fracture Mechanics. Edward Arnold Publ, Delft
138. Lin I H (1983) Mater Sci Lett 2:295
139. Rice J R (1992) J Mech Phys Solids 40:239–271
140. Gorgas I (1986) Scr Metall 20:113–117
141. Hora P, Pelikán V, Machová A, Spielmannová A, Prahl J, Landa M, Červená O (2008) Engng Fract Mech 75:3612–3623
142. Krenn C R, Roundy D, Cohen M L, Chrzan D C, Morris J W Jr (2002) Phys Rev B 65:134111
143. Göken M, Kempf M, Nix W D (2001) Acta Mater 49:903–911

144. Göken M, Kempf M (2001) Z Metallkd 92:1061–1067
145. Horníková J, Černý M, Šandera P, Pokluda J (2007) Acta Metall Slov 13:65–69
146. Horníková J, Černý M, Šandera P, Pokluda J (2007) Key Engng Mater 348/349:8001–8004
147. Bei H, Lu Z P, George E P (2004) Phys Rev Lett 93:125504
148. Horníková J, Šandera P, Černý M, Pokluda J (2008) Engng Fract Mech 75:3755–3762
149. Pokluda J, Kroupa F, Obdržálek L (1994) Mechanical properties and structure of solids. PCdir, Brno (in Czech)
150. Dekker A J (1957) Solid State Physics. Prentice-Hall, New Jersey USA
151. Jokl M L, Vitek V, McMahon C J Jr, Burgers P (1989) Acta Metall 37:87–97
152. Pokluda J, Vitek V (1999) Metall Mater 37:67–70
153. Wnuk M P (1974) J Appl Mech 41:234–242
154. Neimitz A, Aifantis E C (1987) Engng Fract Mech 26:505–518
155. Unger D J, Aifantis E C (1983) Acta Mech 47:117–151
156. Cottrell A H (1953) Dislocations and Plastic Flow in Crystals. Oxford University Press, Oxford
157. Hahn G T, Rosenfield A R (1975) Metall Trans A6:653–668
158. Kroupa F, Vitek V (1967) Can J Phys 45:945–971
159. Felkins K, Leighly H P Jr, Jankovic A (1998) J Metals 50:12–18
160. Hondros E D, Seah M P, Hofmann S, Lejček P (1996) Interfacial and surface microchemistry. In: Cahn R W, Haasen P (eds) Physical Metallurgy, 4th edition, Chapter 13. North-Holland, Amsterdam
161. Kalderon D (1972) Proc Inst Mech Eng 186:341–375
162. Broek D (1982) Elementary engineering fracture mechanics. Martinus Nijhooff Publ, Dordrecht
163. Anderson T L (1995) Fracture Mechanics. Fundamentals and Applications. CRC Press, Texas
164. Magill M A, Zwerneman F J (1997) Engng Fract Mech 56:9–24
165. Ritchie R O (1988) Mat Sci Eng A103:15–28
166. ASTM E 399-72 Standard method of test for plane-strain fracture toughness of metallic materials
167. Pokluda J (2001) Mechanika 67:277–296
168. Pokluda J, Šandera P, Horníková J (2004) Fat Fract Engng Mater Struct 27:141–157
169. Faber K T, Evans A G (1983) Acta Metall 31:565–576
170. Murakami Y (ed) (1987) Stress Intensity Factors Handbook: Vol 1. Pergamon Books
171. Pokluda J, Podrábský T, Slámečka K, Pospíšilová S, Chai G C (2008) Mater Sci Forum 567/568:101–104
172. Ingrafea T *et al.* (1996) FRANC3D, 3D FRacture ANalysis Code. The Cornell University Fracture Group, Cornell University, Ithaca NY
173. Pokluda J, Šandera P, Horníková J (2005) J ASTM International 2:1–15
174. Chawla K K (1993) Ceramic Matrix Composites. Chapman and Hall, London
175. Boccaccini A R (2001) J Ceram Soc Jap 109:99–109
176. Boccaccini A R, Trusty P A (1996) J Mat Sci Lett 15:60–62
177. Pokluda J, Švejcar J (1999) Structural analysis of fatigue crack growth in ferritic ductile iron. In: Miannay D, Costa P, Francois D, Pineau A (eds) Fatigue 99. EMAS, Beijing
178. Horníková J, Šandera P, Pokluda J (2005) Mater Sci Forum 482:311–314
179. Todd R I, Boccaccini A R, Sinclair R, Yalle R B, Young R B (1999) Acta Mater 47:3233–3240
180. Boccaccini A R, Winkler V (2002) Composites Part A33:125–131
181. Lange F F (1971) J Am Ceram Soc 54:614–20

182. Chaim R, Talanker V (1995) J Am Ceram Soc 78:166–72
183. Horníková J, Šandera P, Pokluda J (2006) Modelling Crack-Tip Shielding Effects in Particle Reinforced Composites. In: Gdoutos E (ed) 16th European Conference of Fracture. Springer
184. Kotoul M, Pokluda J, Šandera P, Dlouhý I, Chlup Z, Boccacini A R (2008) Acta Mater 56:2908–2918
185. Winn A J, Boccaccini A R, Imam N, Trusty P A (1997) J Microscopy 186:35–40
186. Knott J F(1983) Mechanics of Fracture. In: Latanision R M, Pickens J R (eds) Atomistics of Fracture, Plenum Press, New York
187. Kerlins V (1994) Modes of Fracture. In: Mills K *et al.* (eds) ASM Handbook: Vol 12 Fractography. ASM International
188. Šandera P, Ponížil P, Pokluda J (1997) Three dimensional model of intergranular crack development in the process zone. In: Parilák L' (ed) Fractography '97. ÚMV SAV, Stará Lesná
189. Pokluda J, Saxl I, Šandera P, Ponížil P, Matoušek M, Podrábský T, Horníková J (2000) Real-like polycrystal with intergranular crack. In: Miannay D, Costa P, Francois D, Pineau A (eds) Advances in Mechanical Behaviour, Plasticity and Damage, Euromat 2000. Elsevier
190. Walin K (2008) The Use of the Master Curve in Structural Integrity Assessment. In: Pokluda J, Lukáš P, Šandera P, Dlouhý I (eds) Multilevel Approach to Fracture of Materials, Components and Structures (ECF17). VUTIUM, Brno
191. Kim Y J, Lin G, Cornec A, Schwalbe K H (1996) Int J Fract 78:21–34
192. Suresh S (1998) Fatigue of materials. Cambridge University Press, Cambridge, UK
193. Zeman J, Rolc S, Buchar J, Pokluda J (1990) Microstructure and fracture toughness of cast and forged ultra-high-strength, low-alloy (UHSLA) steels. In: Gudas J P, Joyce J A, Hackett E M (eds) Fracture Mechanics: Twenty-First Symposium, ASTM STP 1074. ASTM, Philadelphia, PA
194. Petit J (1998) Metall Mater 3:220–232
195. Cook J R, Irwing P E, Booth G S, Beewers C J (1975) Engng Fract Mech 7:67–77
196. Pokluda J, Siegl J (1990) Fat Fract Engng Mater Struct 13:375–385
197. Kunz L, Lukáš P (1982) Fatigue crack growth in 15CH2NFA steel. In: Karel V (ed) Fractography '82. DT, Žilina, Czechoslovakia (in Czech)
198. Kolednik O (2000) Int J Sol Struct 37:781–808
199. Sun Z, de los Rios E R, Miler K (1991) Fat Fract Engng Mater Struct 14:277–292
200. Pokluda J, Šandera P, Horníková J (2000) Statistical model of roughness-induced crack closure. In: Fuentes M, Elices M, Martín-Meizoso A, Martínez-Esnaola J M (eds) Fracture mechanics: applications and challenges, ECF 13. Elsevier
201. Saltykov C A (1970) Stereometric metallography. Metalurgija, Moscow (in Russian)
202. Saxl I, Ponížil P (1998) Acta Stereol 17:247–252
203. Avery I, Hall F R, Sturgess C E N (1998) J Mater Proc Techn 80/81:565–571
204. Pokluda J, Šandera P, Pippan R (2006) Analysis of crack closure level in terms of crack-wake plasticity. In: Johnson W S (ed) Fatigue 06, Elsevier, Atlanta, Georgia
205. Lee S, Maino L, Asaro R J (1985) Metal Trans 16A:1633–1648
206. Tomita Y (1988) Metal Trans 19A:2313–2321
207. Datta K P, Wood W E (1981) J Test Evaluation 9:111–117
208. Guimaraes R, Savedra A (1985) Metall Trans 16A:329–336
209. Server W L (1992) Charpy impact testing. In: Newby J R *et al.* (eds) ASM Handbook: Vol. 8 – Mechanical Testing

210. Pokluda J, Šandera P, Zeman J (1992) Effect of intergranular crack branching on fracture toughness evaluation. In: Ernst H A, Saxena A, McDowell D L (eds) Fracture Mechanics: Twenty-Second Symposium, ASTM STP 1131. ASTM, Philadelphia PA
211. Šandera P, Pokluda J (1992) Computer simulation of intergranular crack branching. In: Aliabadi H M, Cartwright D J, Nisitani H (eds) Localized Damage 92. CMP Elsevier, Southampton-Boston-London-New York
212. Šandera P, Pokluda J (1996) Metall Mater 34:230–240 (in Czech)
213. Pokluda J, Vlach B, Šandera P, Jurášek L (2001) Antagonism in Fracture and Notch Toughness of UHSLA Steels. In: Francois D, Pineau A (eds) Charpy Centenary Conference SF2M. Les Fontelles, France
214. Underwood E E, Banerjee K (1992) Quantitative fractography. In: Mills K *et al.* (eds) ASM Handbook: Vol. 12 – Fractography. ASM International, Metals Park, Ohio, USA
215. Janovec J, Jenko M, Lejček P, Pokluda J (2007) Mater Sci Eng A462:441–445
216. Lejček P (1994) Anal Chim Acta 297:165–178
217. Lejček P, Pokluda J, Šandera P, Horníková J, Vlach B, Jenko M (2008) Fracture Behavior of Phosphorus-Doped Polycrystalline Fe-2.3%V Alloy. In: Pokluda J, Lukáš P, Šandera P, Dlouhý I (eds) Multilevel Approach to Fracture of Materials, Components and Structures (ECF17). VUTIUM, Brno, Czech Republic
218. Lejček P, Hofmann S, Janovec J (2007) Mater Sci Eng A 462:76–85
219. Wu S J, Ding R G, Knott J F (2007) Mater Sci Technol 23:1262–1268
220. Janovec J, Pokluda J, Jenko M, Lejček P, Vlach B, Horníková J (2006) Surf Interf Anal 38:401–405
221. McClintock F A (1968) J Appl Mech 35:362–371
222. Rice J R, Tracey D M (1969) J Mech Phys Solids 17:201–2017
223. Gurson A L (1977) J Engng Mater Techn 99:2–15
224. Tvergaard V (1981) Int J Fract 17:389–407
225. Staněk P, Pokluda J (1980) Metall Mater 18:709–720 (in Czech)
226. Staněk P, Pokluda J (1983) Metall Mater 21:383–395 (in Czech)
227. McClintock F A (1969) Ductile Fracture. In: Argon A S (ed) Physics of Strength and Plasticity. MIT Press, Cambridge, MA
228. Brown L M, Emburry J D (1973) Inst Metals 1:164–169
229. Rousselier G (1987) Nucl Engng Design 105:97–111
230. Tvergaard V, Needleman A (1984) J Mech Phys Solids 32:461–490
231. Argon A S, Im J, Safoglu R (1975) Metall Trans A6:825–834
232. Lui M W, LeMay I (1976) Eng Mat Techn 4:179
233. Jonas J J, Baudelet B (1977) Acta Metall 25:43–50
234. Staněk P, Pokluda J (1979) On the mechanism of ductile fracture in metalic materials. In: Staněk P, Pokluda J (eds) Prediction of Mechanical Properties of Metallic Materials from Structural Characteristics (Prediction79). DT, Brno (in Czech)
235. Staněk P, Pokluda J (1980) Metall Mater 18:471–481 (in Czech)
236. Gilman J J (1968) Micromechanics of Flow in Solids. Mc Craw-Hill, New York
237. Argon A S, Im J, Needleman A (1975) Metall Trans A6:815–824
238. Bridgman P W (1975) Studies in Large Plastic Flow and Fracture. Mc Craw-Hill, New York
239. De Gennes P Q (1978) Czech J Phys A28:549 (in Czech)
240. Smirnov-Aljajev G A (1961) Resistance of Materials to Plastic Deformation. Metallurgia, Moscow (in Russian)
241. Staněk P, Pokluda J (1984) Metall Mater 22:710–719 (in Czech)
242. Kraft J M, Irwin G R (1965) ASTM STP 381:84–113
243. Rice J R, Johnson M A (1970) The Role of Large Crack Tip Geometry Changes in Plane Strain Fracture. In: Kanninen M F *et al.* (eds) Inelastic Behavior of Solids, McGraw-Hill, New York

244. Hancock J W, Cowling M J (1980) Metal Sci 14:293–304
245. Pokluda J, Šandera P (1990) A Simple method for Calculation of K_{Ic} values of Ductile Materials. In: Koutsky *et al.* (eds) Brittle Fracture of Materials and Structures. Skoda, Pilsen, Czechoslovakia (in Czech)
246. McEvily A (2002) Metal Failures: Mechanisms, Analysis, Prevention. John Viley, New York
247. Miller K J (1993) Mat Sci Technology 9:453–462
248. Zapfe C A, Clogg M Jr (1945) Trans ASM 34:71–107
249. Underwood E E, Banerjee K (1992) Fractal analysis of fracture surfaces. In: Mills K *et al.* (eds) ASM Handbook: Vol 12 – Fractography. ASM International, Metals Park, Ohio, USA
250. Dong W P, Sullivan P J, Stout K J (1994) Wear 178:29–43
251. Gadelmawla E S, Koura M M, Maksoud T M A, Elewa I M, Soliman H H (2002) J Mater Proc Tech 123:133–45
252. Suh A Y, Polycarpou A A, Conry T E (2003) Wear 255:556–568
253. Bakolas V (2003) Wear 254:546–554
254. Sherrington I, Howarth G W (1998) Int J Mach Tool Manufact 38:599–606
255. Okabe A, Boots B, Sugihara K (1992) Spatial Tessellations: Concepts and Applications of Voronoi Diagrams. Wiley, New York
256. Petropoulos G P, Vaxevanidis N M, Pandazaras C N, Antoniadis A T (2004) Wear 257:1270–1274
257. Geometrical Demands on Production (GPS) – Surface Structure: Profile Method – Terms, Definitions and Parameters. CSN EN ISO 4287, 1999 (in Czech)
258. Wang S H, Müller C (1998) Mater Sci Eng A255:7–15
259. Mandelbrot B B (1984) The Fractal Geometry of Nature. Freeman, New York
260. Balankin A S (1997) Engng Fract Mech 57:135–203
261. Camastra F (2003) Pattern Recogn 36:2945–2954
262. Zaiser M, Bay K, Hahner P (1999) Acta Mater 47:2463–2476
263. Xie H, Wang J (1999) Int J Sol Struct 36:3073–3084
264. Yuan C Q, Li J, Yan X P, Peng Z (2003) Wear 255:315–326
265. Charkaluk E, Bigerelle M, Iost A (1998) Engng Fract Mech 61:119–139
266. Campos I, Balankin A S, Bautista O, Ramirez G (2005) Theor Appl Fract Mech 44:187–191
267. Guerrero C, Reyes E, Gonzalez (2002) Polymer 43:6683–6693
268. Weiss J (2001) Engng Fract Mech 68:1975–2012
269. Pokluda J, Staněk P (1980) Strojirenstvi 30:485–496 (in Czech)
270. Antolovich S D, Saxena A (1992) Fatigue Failures. In: Powel G W, Mahmoud S E (eds) ASM Handbook: Vol 11 Failure Analysis and Prevention. ASM International
271. Beachem C D (1967) Trans ASM 60:324–343
272. McEvily A (2007) Mater Sci Forum 567/568:397–400
273. Paris P C, Erdogan J (1963) J Basic Eng 85:528–537
274. Rice J R (1967) Mechanics of Crack Tip Deformation and Extension by Fatigue. In: Fatigue Crack Propagation, ASTM STP 415, Philadelphia
275. Petit J, Hanaff G, Sarrazin-Badoux C (2000) Fatigue Crack Threshold, Endurance Limits and Design, In: Newman J C, Piascik R S (eds) ASTM STP 1372, ASTM
276. Lipetzky P, Knésl Z (1995) Int J Fract 73:81–92
277. Simha N K, Fischer F D, Kolednik O, Chen C R (2003) J Mech Phys Solids 51:209–240
278. Pokluda J, Staněk P (1985) Scr Metall 19:435–439
279. Pokluda J (1994) Mater Engng 1:21–29 (in Czech)
280. Menčík J. (1994) Strength and Fracture of Mass and Ceramics. SNTL, Prague (in Czech)

281. Polák J, Klesnil M (1982) Fat Fract Engng Mater Struct 5:19–32
282. Kenedy A J (1953) Nature 71:927–928
283. Benham P P (1961) J Inst Mater 89:328–338
284. Elfmark J, Pokluda J, Staněk P (1980) Jader Energ 10:361–374 (in Czech)
285. Bezděk L *et al.* (1973) Fatigue Fractures of Military Steels and Components. Res Rep IA17-73, Military Academy, Brno (in Czech)
286. Pokluda J, Staněk P (1978) Kovove Mater 16:583–598 (in Czech)
287. Pokluda J (1984) On the cyclic creep of metalic materials. PhD Thesis, Masaryk University, Brno (in Czech)
288. Bartík L, Pokluda J (1998) Metall Mater S36:53–56
289. Klesnil M, Lukáš P (1975) Fatigue of metallic materials under cyclic loading. Academia, Prague (in Czech)
290. Pokluda J, Staněk P (1980) Probl Prochn 9:16–29 (in Russian)
291. Lorenzo F, Laird C (1984) Acta Metall 32:671–680
292. Oldroyd P W J, Radon J C (1979) Fatigue Fract Engng Mater Struct 1:297–306
293. Mròz Z (1969) Acta Mechanica 7:199–212
294. Dafalias Y F, Popov E P (1975) Acta Mechanica 21:1973–1992
295. Pokluda J, Staněk P (1982) Kovove Mater 20:521–523 (in Czech)
296. Bartík L (1999) Mechanical properties of ultra high-strength steels of the Czech provenience. PhD Thesis, Brno University of Technology, Brno (in Czech)
297. Mughrabi H (1985) (ed) Dislocations and Properties of Real Materials, The Institute of Metals, London
298. Stroh, A N (1957) Adv Phys 6:418–465
299. Tanaka K, Mura T (1981) J Appl Mech 48:97–103
300. Liu W, Bayerlein M, Mughrabi H, Day A, Quested P N (1992) Acta Metall Mater 40:1763–1771
301. Van der Ven A, Ceder G (2004) Acta Mater 52:1223–1235
302. Wejdemann C, Pedersen O B (2004) Mater Sci Eng A 387:556–559
303. Gerold V (1982) Scr Metall 16:405
304. Lukas P, Klesnil M, Krejci J (1968) Phys Stat Sol 27:545–558
305. Finney J M, Laird C (1975) Phil Mag 31:339–366
306. Laird C, Finney J M, Kuhlmann-Wilsdorf D (1981) Mater Sci Eng 50:127–136
307. Kuhlmann-Wilsdorf D, Laird C (1980) Mater Sci Eng A46:209–219
308. Rasmussen K V, Pedersen O B (1980) Acta Metall 14:1467–1478
309. Eshelby J D (1957) Proc Roy Soc London A 241:376–396
310. Sauzay M, Gilormini P (2002) Theor Appl Fract Mech 38:53–62
311. Sauzay M (2009) Influence of Slip Localization on Crack Initiation at the Grain Scale. In: Elboujdaini M (ed) 12th International Conference on Fracture (ICF12). NRC, Ottawa, Canada
312. Polák J (1991) Cyclic Plasticity and Low Cycle Fatigue Life of Metals. Academia, Prague
313. Polák J (1987) Mater Sci Eng A92:71
314. Polák J, Lepistö T, Keitunnen P (1985) Mater Sci Eng A74:85–91
315. Essmann U, Gösselle U, Mughrabi (1981) Phil Mag 44:405–426
316. Antonopoulos J G, Brown L M, Winter A T (1976) Phil Mag 34:549–563
317. Ford F P (1996) Corrosion 52:375–395
318. Miller K J, de los Rios E R (eds) (1986) The behaviour of short fatigue cracks. Mechanical Engineering Publication, London, UK
319. Kitagawa H, Takahashi S (1976) Applicability of fracture mechanics to very small cracks or the cracks in the early stage. In: Promisel N E, Weiss V (eds) Mechanical Behavior of Materials. ASM, Metals Park, OH
320. Riemelmoser F O, Pippan R, Stüwe H P (1998) Acta Mater 46:1793–1799
321. Dai S A, Li J C M (1982) Scr Metall 16:183–188
322. Riemelmoser F O, Pippan R, Kolednik O (1997) Comput Mech 20:139–144
323. Pelloux R M N (1969) Trans Am Soc Met 62:281–89

324. Wanhill R J H (1975) Metall Trans 6A:1587–95
325. Neumann P (1969) Acta Metall 17:1219–25
326. Elber W (1970) Engng Fract Mech 2:37–45
327. Toyosada M, Gotoh K (2005) Mater Sci Forum 482:95–102
328. Suresh S, Ritchie R O (1982) Metall Trans 13A:1627–1631
329. Wang S H, Müller C (1999) Analytical evaluation and experimental study of roughness-induced crack closure. In: Wu X R, Wang Z G (eds) Fatigue 99: Proceedings of the seventh international fatigue congress. Emas, Beijing
330. Noda N, Oda K (2001) Zig-zag Edge Crack in Semi-infinite Plain under Uniaxial Tension. In: Murakami Y (ed) Stress Intensity Factors Handbook: Vol IV. TSMS Elsevier
331. Hanlon T, Suresh S (2005) Fatigue of Nanostructured Metals and Alloys. In: Carpinteri A (ed) International Congress on Fracture (ICF11). Politechnico di Torino, Torino Italy
332. Kondo Y (2005) Mater Sci Forum 482:89–94
333. Pippan R (1993) Engng Fract Mech 44:821–829
334. Slámečka K, Ponížil P, Pokluda J (2007) Mater Sci Eng A462:359–362
335. Horníková J, Šandera P, Pokluda J (2006) Key Engng Mater 324–325:803–806
336. Carter R D, Lee E W, Starke E A Jr, Beevers C J (1984) Metall Trans 15A:555–563
337. Pippan R (1998) Phil Mag 77A:861–873
338. Robinson J L, Beevers C J (1973) Metal Sci J 7:153–159
339. Gregory J K (1996) Fatigue Crack Growth of Titanium Alloys. In: Lampman S R *et al.* (eds) ASM Handbook Fatigue and Fracture: Vol 19. ASM, Metals Park, OH
340. Boyce B L, Ritchie R O (2001) Engng Fract Mechanics 68:129–147
341. Pippan R (1991) Mater Sci Eng A138:1–13
342. Pippan R, Berger M, Stüwe H P (1987) Metall Trans 18A:429–435
343. Shang J K, Tzou J L, Ritchie R O (1987) Metall Trans 18A:1613–1627
344. Taylor D (1989) A Compendium of Fatigue Thresholds and Growth Rates. EMAS, Warley
345. Wang Z G, Al S H (1999) ISIJ Inter 39:747–759
346. Pokluda J, Kondo Y, Slámečka K, Šandera P, Horníková J (2008) Key Engng Mater 385/387:49–52
347. Pook L P (2002) Crack Paths. Wit Press, UK
348. Pokluda J, Pippan R (2005) Fat Fract Engng Mater Struct 28:179–186
349. Nayeb-Hashemi H, McClintock F A, Ritchie R O (1983) Int J Fract 23:163–185
350. Tschegg E K (1982) Mater Sci Eng A 54:127–136
351. Tschegg E K (1983) J Mater Sci 18:1604–1614
352. Tschegg E K (1983) Acta Metall 31:1323–1330
353. Tanaka K, Akinawa Y and Yu H (1999) The propagation of a circumferential fatigue crack in medium-carbon steel bars under combined torsional and axial loadings. In: Miller K J and D L McDowel D L (eds) Mixed-mode Crack Behaviour. ASTM 1359, West Conshohocken, PA
354. Murakami Y, Kusumoto R, Takahashi K (2002) Growth mechanism and threshold of mode II and mode III fatigue crack. In: Neimitz A *et al.* (eds) Fracture Mechanics Beyond 2000 (ECF14). EMAS, UK
355. Murakami Y (2002) Private communications
356. Nayeb-Hashemi H, McClintock F A (1982) Metall Trans A 13:2197–2204
357. Ritchie R O, McClintock F A, Nayeb-Hashemi H, Rittler M A (1982) Metall Trans A 13:101–110
358. Tanaka K (2009) Crack propagation in lead-free solder under cyclic loading of mode I and II. In: Atzori B, Carpinteri A, Lazzarin P, Pook L P (eds) Crack Paths 2009. University of Padua, Vicenza

359. Vaziri A, Nayeb-Hashemi H (2005) Engng Fract Mech 72:617–629
360. Makabe C, Anggit M, Sueyoshi T, Yafuso T (2006) J Test Eval 34:423–429
361. Pokluda J, Slámečka K, Šandera P (2009) On the mechanism of factory-roof formation. In: Atzori B, Carpinteri A, Lazzarin P, Pook L P (eds) Crack Paths 2009. University of Padua, Vicenza
362. Miller K J *et al.* (1985) Multiaxial Fatigue. In: Miller K J, Brown, M W (eds) ASTM STP 853, ASTM, Philadelphia
363. Matake T (1977) Bulet JSME 20:257
364. Vaziri A, Nayeb-Hashemi H (2006) Int J Sol Struct 43:4063–4081
365. Holáň L, Pippan R, Pokluda J, Horníková J, Hohenwarter T, Slámečka K (2009) Near-threshold propagation of Mode II and Mode III cracks. In: Atzori B, Carpinteri A, Lazzarin P, Pook L P (eds) Crack Paths 2009. University of Padua, Vicenza
366. Hellier A K, Corderoy D L H, Mc Girr M B (1987) Int J Fatigue 9:95–101
367. Hellier A K, McGirr M B, Corderoy D J H, Kutajczyk L A (1990) Int J Fract 42:R19–R23
368. Pokluda J, Trattnig G, Martinschitz C, Pippan R.(2008) Int J Fatigue 30:1498–1506
369. Horníková J, Šandera P, Pokluda J (2010) Key Engng Mater 417/418:321–324
370. Slámečka K, Pokluda J (2003) 3D Analysis of Fatigue Fracture Morphology Generated by Combined Bending – Torsion. In: Nilsson F *et al.* (eds) Advanced Fracture Mechanics for Life and Safety Assesments (ECF15). KTH, Stockholm
371. Benthem J P, Koiter W T (1973) Asymptotic approximations to crack problems. In: Sih G C (ed) Method of Analysis and Solutions of Crack Problems. Noordhoff International Publishing, Leyden
372. Lampman S (1996) Fatigue and Fracture Properties of Stainless Steels. In: Lampman S R *et al.* (eds) ASM Handbook Fatigue and Fracture: Vol 19. ASM, Metals Park, OH
373. Sander M, Richard H A (2002) Effects of Block Loading and Mixed Mode Loading on the Fatigue Crack Growth. In: Blom A F (ed) Fatigue 2002. Stockholm, Sweden
374. James M, Herman D J, Scott F (2003) Fatigue crack growth rate and stress intensity factor corrections for out-of-plane crack growth. In: Daniewitz S R, Newman J C, Schwalbe K H (eds) Fatigue and Fracture Mechanics. ASTM, West Conshohocken
375. Socie D F, Marquis G B (2000) Multiaxial fatigue. SAE International, Warrendale
376. Gough H J, Pollard H V (1935) Proc Inst Mech Eng 131:3–103
377. Gough H J (1950) J Appl Mech 50:113–125
378. Sines G (1959) Behavior of Metals Under Complex Statis and Alternating Stresses. In: Sines G, Waisman J L (eds) Metal Fatigue. MsGraw-Hill, New York
379. Crossland B (1956) Effect of large hydrostatic pressure on the torsional fatigue strength of an alloy steel. In: Fatigue of Metals. Institution of Mechanical Engeneers, London
380. Findley W N(1959) J Engng Ind 7:301–306
381. Papadopoulos I V, Davoli P, Gorla C, Filippini M, Bernasconi A (1997) Int J Fatigue 19:219–235
382. McDiarmid D L (1991) Fat Frac Eng Mat Struct 14:429–453
383. Carpinteri A, Spagnoli A (2001) Int J Fatigue 23:135–145
384. Dang Van K (1999) Introduction to Fatigue Analysis in Mechanical Design by the Multiscale Approach. In: Dang Van K, Papadopoulos I V (eds) High-Cycle Metal Fatigue in the Context of Mechanical Design. Springer, Vienna
385. Papadopoulos I V (1998) Fat Frac Eng Mat Struct 21:269–285

386. Gonçalves C A, Araujo J A, Mamiya E N (2005) Int J Fatigue 27:177–187
387. Major Š, Papuga J, Horníková J, Pokluda J (2008) Strength Mater 40:64–67
388. De la Cruz P, Oden M, Ericsson T (1998) Mat Sci Eng A242:181–194
389. Genel K, Demirkol M, Çapa M E (2000) Mat Sci Eng A279:207–216
390. Pokluda J, Dvořák I, Horáková H, Major Š (2006) Influence of Plasma-Nitriding Surface Layer on Fatigue Life of Steel Specimens under Push-Pull and Bending-Torsion. In: Johnson W S (ed) Fatigue 2006. Elsevier, Atlanta, Georgia, USA
391. Carpinteri A, Spagnoli A, Vantadori S (2002) Fat Fract Engng Mater Struct 25:619–627
392. Carpinteri A, Spagnoli A (2004) Int J Fatigue 26:125–133
393. Slámečka K, Pokluda J, Ponížil P, Major Š, Šandera P (2008) Engng Fract Mech 75:760–767
394. Limodin N, Verreman Y (2006) Mat Sci Eng A435/436:460–467
395. Sirin S Y, Sirin K, Kaluc E (2008) Mat Charact 59:351–358
396. Murakami Y (2001) Mechanism of fatigue silure in ultralong life regime. In: Stanzl-Tschegg S, Mayer H (eds) Fatigue in the very high cycle regime. Institute of Metrology and Physics, Vienna, Austria
397. Terentev V F (2004) Metal Sci Heat Treat 46:244–249
398. Kuroshima Y, Harada S (2001) Fatigue crack growth mechanism of high strength steel in gigacycle fatigue region. In: Stanzl-Tschegg S, Mayer H (eds) Fatigue in the very high cycle regime. Institute of Metrology and Physics, Vienna, Austria
399. Murakami Y (2002) Metal Fatigue: Effects of Small Defects and Nonmetallic Inclusions. Elsevier, Oxford, UK
400. Shiozawa K, Lu L T (2001) Superlong fatigue behaviour of shot-peened high-strength steel, In: Stanzl-Tschegg S, Mayer H (eds) Fatigue in the very high cycle regime. Institute of Metrology and Physics, Vienna, Austria
401. Gong Y, Norton M P (1996) J Test Eval 24:263–267
402. Slámečka K, Pokluda J, Kianicová M, Major Š, Dvořák I (2010) Int J Fatigue 32:921–928
403. Onuki A, Yanagi N, Satoh N, Takase F (1992) Fatigue strength of a ion nitrided steel. In: Sedmak (ed) 9th European Conference on Fracture (ECF9). Varna, Bulgaria
404. Holemář A, Hrubý V (1989) Ion nitriding in the practice. SNTL, Prague (in Czech)
405. Forsyth P J E, Ryder D A (1960) Aircraft Engng 32:96–99
406. Jacoby G (1965) Exper Mech 5:65–82
407. Peel C J (1972) An Analysis of a Test Fatigue Failure by Fractography and Fracture Mechanics. Royal Aircraft Establishment, TR 72034
408. Ryder D A, Bunk W (1974) Zeit Flugwiss 22:223
409. Uchimoto T, Sakamoto A, Nagata S (1977) Trans ISIJ 17:1
410. Pokluda J, Staněk P (1981) Probl Prochn 4:13–20 (in Russian)
411. Pokluda J, Staněk P (1981) Acta Techn 4:415–428
412. Nedbal I, Siegl J, Kunz J, Lauschmann H (2008) Fat Fract Engng Mater Struct 31:164–176
413. Nedbal I, Lauschmann H, Siegl J, Kunz J (2008) Fat Fract Engng Mater Struct 31:177–183
414. Staněk P, Pokluda J, Kopeček K (1980) Strojírenství 30:681–686
415. Pokluda J, Staněk P, Unčovský A (1984) Failure of Compressor Rotor of Aircraft Engine M-301. Res Rep VU23-84, Military Research Institute 070, Brno (in Czech)
416. Pokluda J, Šandera P (2006) Simple Method for Estimation of Fatigue Loading and Useful Life from Fracture Morphology. In: Carpinteri A (ed) 11th International Conference on Fracture (ICF11). Torino, Italy

417. Forman R G, Kearney V E, Engle R M (1967) J Basic Engng 89:459–470
418. Klesnil M, Lukáš P (1972) Engng Fract Mech 4:77–92
419. Murakami Y *et al.* (1987) Stress Intensity Factors Handbook. Pergamon Press, Oxford-New York
420. Prokopenko A V (1981) Probl prochn 4:105 (in Russian)
421. Thomas L H (1927) Proc Cambr Phil Soc 23:542–548
422. Slater J C (1951) Phys Rev 81:385–390
423. Hartree D R (1928) Proc Cambr Phil Soc 89:426–437
424. Ceperley D M, Alder B J (1980) Phys Rev Lett 45:566–569
425. Perdew J P, Wang Y (1986) Phys Rev B33:8800–8802
426. Perdew J P, Burke K, Wang Y (1996) Phys Rev B54:16533–16539
427. Ziesche P, Kurth S, Perdew J P (1998) Comp Mater Sci 11:122–127
428. Andersen O K (1975) Phys Rev B12:3060–3083
429. Andersen O K (1981) Europhys News 12:4–8
430. Skriver H L (1983) The LMTO Method: Muffin-Tin orbitals and Electronic Structure. Springer Verlag, Berlin
431. Krier G, Jepsen O, Burkhardt A, Andersen O K (1994) The LMTO-ASA program. Max-Planck Institut für Festkörperforschung, Stuttgart
432. Andersen O K, Jepsen O (1984) Phys Rev Lett 53:2571–2574
433. Blaha P, Schwarz K, Madsen G, Kvasnicka D, Luitz J (2001) WIEN2k Users Guide. Vienna University of Technology, Vienna, Austria
434. Blaha P, Schwarz K, Luitz J (1997) A Full Potential Linearized Augmented Plane Wave Package for Calculating Crystal Properties. Vienna University of Technology, Vienna
435. Singh D J (1994) Planewaves Pseudopotentials and the LAPW Method. Kluwer Academic Publishers, Boston-Dordrecht-London
436. Kresse G, Hafner J (1994) J Phys Cond Matter 6:8245–8257
437. Vanderbildt D (2003) Phys Rev B67:104105
438. Blöchl P E (1994) Phys Rev B50:17953–17979
439. Sih G C J (1973) Engng Fract Mech 5:365–377
440. Richard H A, Fulland M, Schöllmann M, Sander M (2002) Simulation of Fatigue Crack Growth using ADAPTCRACK3D. In: Blom A F (ed) Fatigue 2002. EMAS, Stockholm
441. Gurland J, Plateau J (1963) Trans ASM 56:442–454
442. Cox T B, Low J R (1974) Metall Trans 6A:1457–1470
443. Bergh S (1962) Jemkont Allnaler 146:748–762
444. Kleverbring B I, Bogren E, Mahrs R (1975) Metall Trans 6A:319–327
445. Staněk P, Pokluda J (1978) On the theory of ductile fracture in metals. In: Staněk P, Pokluda J (eds) Prediction of Mechanical Properties of Metallic Materials from Structural Characteristics (Prediction78). DT, Brno (in Czech)

Index

C

N

O

T